QCD Tests at LEP and SLC

Klaus Hamacher[a] *

[a]Fachbereich Physik, Bergische Universität Wuppertal,
Gauß–Straße 20, 42329 Wuppertal, Germany

During the era of LEP and SLC many precison tests of QCD have been performed. This talk summarises some important results.

1. The energy evolution of event shape means – The QCD β–function

The study of event shape observables provides a classical path for determinations of the strong coupling α_s (for an overview see [1]). Besides by the radiation of hard gluons from the initial $\mathrm{q\bar{q}}$ state the event shape is influenced by the non-perturbative hadronisation process including final state mass effects.

The energy evolution of event shape observables, in the simplest case of their mean values (in the following for brevity called shape means) in principle allows to assess the perturbative and non-perturbative contributions to the event shape. The evolution of the perturbative part is related to the QCD β–function describing the energy evolution of the coupling. This evolution is directly linked to the quantum effects generating the scale of strong interaction physics and the experimentally observed properties of asymptotic freedom and confinement. The influence of the non-perturbative hadronisation is expected to vanish as the inverse power of the energy. This is intuitively understood assuming the average transverse momentum of a hadron due the hadronisation to be constant and uncorrelated with the perturbative process. Here transverse momenta increase (up to logarithmic corrections) proportional to the energy of the process leading finally to the $1/E$–decrease of the relative importance of the hadronisation. This behaviour of the hadronisation process is presumably related to the infrared renormalons appearing in perturbation theory (for more explanations and references on "power" corrections see [2])

The energy evolution of a shape mean $\langle f \rangle$ can be effectively described by the simple ansatz[3]:

$$\langle f \rangle = \langle f \rangle_{pert.} + \frac{C_f}{E_{CM}} \qquad \text{with} \qquad (1)$$
$$\langle f \rangle_{pert.} = A_f \bar{\alpha}(\mu) + (A_f \beta_0 \ln x_\mu + B_f) \bar{\alpha}^2(\mu) \ .$$

Where $\bar{\alpha} = \alpha_s/2\pi$ and $x_\mu = \mu/E_{CM}$ is the renormalisation scale factor appearing due to the truncation of the perturbative series. The perturbative coefficients A_f and B_f are usually provided in the $\overline{\mathrm{MS}}$–scheme. The fitted constant C_f measures the size of the non-perturbative contribution. More elaborate models relate the power terms of different observables f perturbatively to a parameter α_0 which is presumed to be universal. The successful description of the data by power models (see [2]) alone does not provide compelling evidence for genuine power terms, however. Power terms are subject to ambiguities. They depend on the borderline between perturbative and non-perturbative physics which is a matter of convention. In fact a strong correlation between the size of C_f and the second order perturbative coefficient B_f (see Fig. 1) is observed[3]. This indicates that the fitted "non-perturbative" term C_f may largely result from higher order perturbative contributions.

This conjecture is inforced by a comparison of the data on shape means to so called Renormalisation Group Invariant (RGI) perturbation theory. The corresponding theoretical work [4,5] dates back to 1982. Simple RGI is valid only for

*E-mail: klaus.hamacher@physik.uni-wuppertal.de

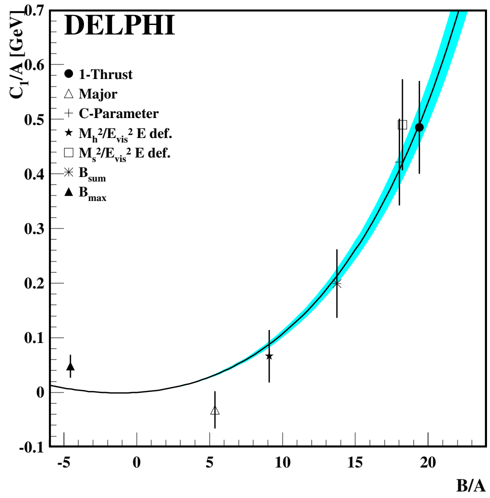

Figure 1. Correlation of the fitted parameter C_f with the second order perturbative coefficient B_f for seven observables. Both parameters are normalised to the first order coefficient A_f to ease the comparison of different observables. The shaded band shows the prediction from RGI for $\Lambda_{\overline{\rm MS}} = 220 - 280$MeV.

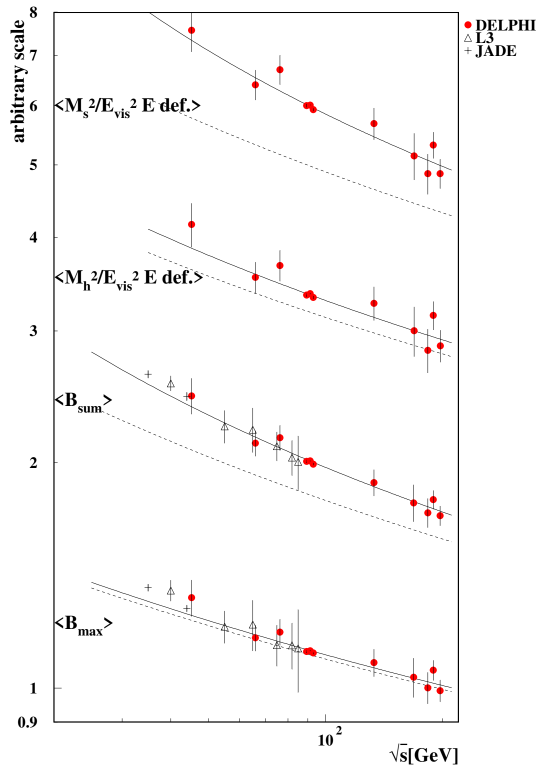

Figure 2. Comparison of RGI predictions (full lines) to data on shape means. Predictions with and without power terms are indistinguishable. The dashed line shows the $\overline{\rm MS}$–prediction for the same value of $\Lambda_{\overline{\rm MS}}$.

observables R depending on a single energy scale like shape means or total cross–sections. The observables are normalised to their leading order perturbative coefficient, i.e. $R = \langle f \rangle / A_f$. RGI demands the observable to fulfill the Renormalisation Group Equation, RGE:

$$Q^2 \frac{dR}{dQ^2} = -\beta_0 R^2 (1 + \rho_1 R + \rho_2 R^2 \ldots) = \rho(R) \quad (2)$$

and so derives scheme independent predictions. It is shown that β_0 $(= (11C_A - 2n_f)/3)$ and the coefficients ρ_i are scheme invariant. β_0 and ρ_1 are identical to the coefficients appearing in the β-function of α_s. Therefore the solution of Eqn.2 is equivalent to the implicit equation for α_s.

$$\frac{\beta_0}{2} \ln \frac{Q}{\Lambda_R} = \frac{1}{R} - \rho_1 \ln \left(1 + \frac{1}{\rho_1 R}\right) + \ldots \quad (3)$$

In NLO the higher order terms indicated by $\ldots$ in Eqn.3 vanish. The integration constant Λ_R is an R-specific scale parameter. Λ_R can be converted into $\Lambda_{\overline{MS}}$ without any loss of precision using the so called Celmaster Gonsalves equation [6].

Power corrections can be included into RGI by a modification of the ρ function [7,8]:

$$\rho(x) \longrightarrow \rho(x) - \frac{2K_0}{\beta_0} x^{\frac{2\rho_1}{\beta_0}} e^{\frac{2}{\beta_0 x}} \quad (4)$$

Where $K_0 \propto C_f$ is a free parameter determining the size of the non–perturbative correction.

RGI predictions with and without additional power terms have been compared to data on mean values of seven shape observables in [3]. Here observables have been chosen which are insensitive to mass terms and a small correction for b-mass effects has been applied [2]. RGI predictions are observed to describe the data very well (see e.g.

[2]This differs to a comparison to data on $\langle 1 - T \rangle$ in [8].

Fig. 2). Power terms are insignificant, consistent with zero. From a comparison of the fits with and without power terms the typical size of the power terms may be of $\mathcal{O}(2\%)$ at Z energies. The agreement of the α_s values obtained from the observables with strongly differing higher order corrections (compare B coefficients in Fig. 1) is very good. Neglecting power terms

$$\alpha_s(M_Z) = 0.1201 \pm 0.0020_{RMS} \pm 0.0003_{syst.} \quad (5)$$

is obtained as a simple mean. The RMS error specifies the small scatter of the individual results. Provided the possible presence of power terms is clarified the good stability of the results for α_s indicates a possibility for measurements of the strong coupling with increased precision using RGI.

Setting Eqn. 1 equal to the RGI prediction the expected size of the power term C_f/E_{CM} can be estimated. The result agrees well with the measurements (see shaded band in Fig. 1). Similarly estimates for the non–perturbative parameter α_0 (for references see [2]) can be obtained. The RGI estimates follow the data much better than a presumed universal value of α_0 [3].

As the β–function itself is not fixed by the RGI approach Eqn. 2 opens a way for a direct measurement of the QCD β–function. Rewriting Eqn. 2 yields:

$$\frac{dR^{-1}}{d\ln Q^2} = -\beta_0 - \frac{1}{2}\beta_1 R + \ldots \quad (6)$$

Thus the β–function is the logarithmic energy slope of the inverse of the shape observable mean. Correcting for the small second term of the β–function

$$\langle\beta_0\rangle = 7.7 \pm 0.9 \pm 0.1_{syst} \pm 0.1_{b-mass} \quad (7)$$

has been obtained from seven observables [3]. The uncertainty of b-mass correction is estimated by a 20% variation of the correction. This result should be compared to the value $7\frac{2}{3}$ expected from QCD.

In order to reduce the uncertainty on the β–function measurement data on $\langle 1-\mathrm{T}\rangle$ at low energies has been included (see Fig. 3) leading to

$$\beta_0 = 7.86 \pm 0.32 \qquad n_f = 4.75 \pm 0.44 \quad . \quad (8)$$

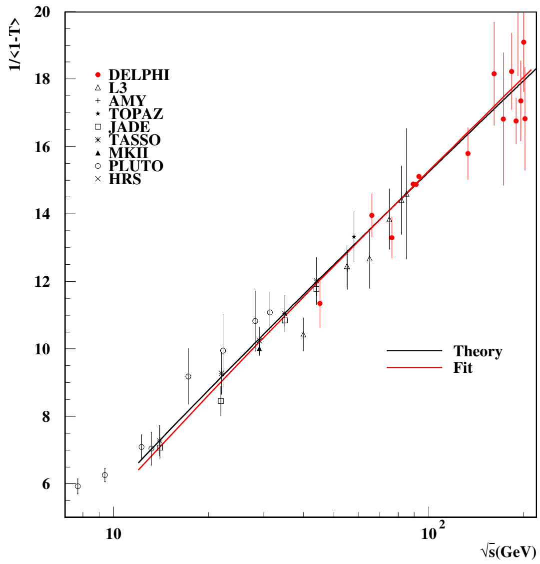

Figure 3. Determination of the β–function from a fit to data on $\langle 1 - \mathrm{Thrust}\rangle$

Here the value of n_f has been determined alternatively to β_0 assuming QCD relations. The specified uncertainties include estimates of the experimental systematics. Uncertainties due to obscure power terms are neglected, however. A relative power term contribution of 2% at the Z induces about an 1.5% shift in the beta function. Still the above result closes the remaining window for hypothetical light gluinos[9].

2. The Running of the b–Quark Mass

Quarks are not asymptotic states of QCD. Hence quark masses can only be indirectly determined by their influence on hadron or hadronic properties. Beside the intuitive perturbative pole mass definition the so called running mass $m_b(\mu)$ is customarily used. This definition treats a mass like an additional coupling which needs to be renormalised, leading to a scale dependent running mass. The scale dependence of m_q is regulated by the so called γ–function:

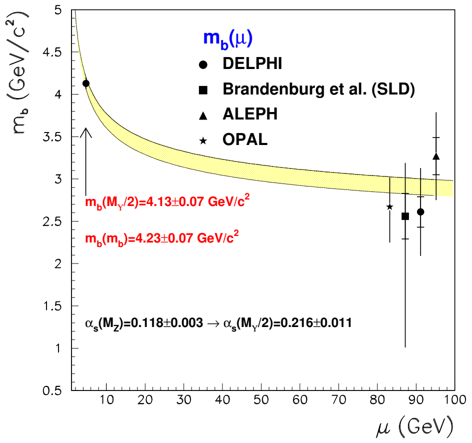

Figure 4. Measurements of the b quark mass $m_b(\mu)$ at different energy scales μ compared to the expected running[14].

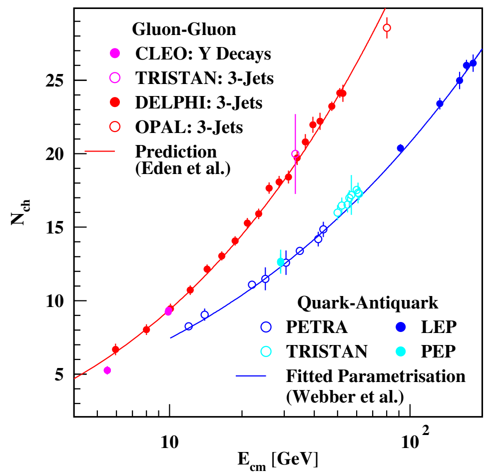

Figure 5. Comparison of the multiplicity of colour singlet gg events to q$\bar{\mathrm{q}}$ events as function of the centre–of–mass energy.

$$\mu\frac{dm_q}{d\mu} = -m_q \cdot \gamma(\alpha_s)$$
$$= -m_q \cdot \left(\gamma_1\frac{\alpha_s}{\pi} + \gamma_2\left(\frac{\alpha_s}{\pi}\right)^2 + \ldots\right) \quad (9)$$

The running of the b–quark mass is experimentally accessible from a comparison of measurements from bound states at low scale and the three jet rate of b events at the Z. Here the reduction of the three jet rate due to the increased quark mass in b events is measured in comparison to light quark events. Quark tagging is efficiently performed using impact parameter tags. Experimental biases as well as hadronisation effects are corrected for using Monte Carlo techniques.

Results for $m_{\mathrm{b}}(M_{\mathrm{Z}})$ fall close to 3 GeV (see Fig.4) nicely confirming the mass running expected from QCD. Statistical precision of $\mathcal{O}(5\%)$ has been reached by the LEP experiments[10–12] [3] and SLD[13]. Dominant uncertainties are due to theoretical ambiguities and limited knowledge of the hadronisation process estimated e.g. by comparison of different hadronisation models. It can, however, be shown that the hadronisation uncertainty is reduced when restricting to regions of the phase–space where the models describe the dynamical distributions of b–hadrons well[14].

[3] The 1% measurement by OPAL presuming anti–correlation of observables lies below the minimum variance bound estimated for the quoted statistics.

3. Measurements of Colour Factors

Colour factors are the eigenvalues of the Casimir operators of the group underlaying a gauge theory. Knowing the colour factors is equivalent to knowing the gauge group. As terms proportional to the Casimir operators appear in the cross-sections the colour factors can be measured from data. The cross-section for gluon bremsstrahlung from quarks is $\propto C_F$, that for bremsstrahlung from gluons (that is the triple gluon vertex) is $\propto C_A$. Pairproduction of a quark-antiquark pair is $\propto T_F$. In contrary to bremsstrahlung the latter process is not collinear/IR divergent. Therefore it is of subordinate importance in the evolution of parton showers.

Maybe the most direct access to the colour factor ratio $C_A/C_F(= 9/4)$ comes from the comparison of the hadron multiplicity in gluon to quark jets. Naively it is expected to directly yield the colour factor ratio. However, experimental measurements only yield ratios between 1.1 and 1.5 (see e.g. [15]). Recent work lead to the under-

standing of this discrepancy:
– Lorentz invariance and colour coherence cause the transverse momentum of a jet to be the relevant scale for its evolution. Considering these scales the multiplicity of a three jet event can be described as the sum of the multiplicity of a q$\bar{\mathrm{q}}$ system at reduced centre–of–mass energy and half of the multiplicity of a gg event at $\sim 2p_\perp^g$.
– The selection of a three jet event at a given y_{cut} constitutes a bias to the underlaying jets as non of the jets may contain particles leading to y values larger than y_{cut}.
– Finite energy effects cause a severe correction to the above naive expectation for the multiplicity ratio. This correction is described by the following differential equation for the energy evolution of the multiplicity in gluon and quark jets[17]:

$$\left.\frac{dN_{gg}(L')}{dL'}\right|_{L'} = \frac{C_A}{C_F}\left(1-\frac{\alpha_0 c_r}{L}\right)\frac{d}{dL}N_{q\bar{q}}(L) \qquad (10)$$

$$L = \log\frac{s}{\Lambda^2}\ ,\ L' = L + c_g - c_q\ ,\ c_i = \mathrm{const.}$$

Integration of this equation leads to a non-perturbative constant accounting for differences in the fragmentation of gluon and quark jets. From a comparison of the slope of the multiplicity of symmetric three jet events with increasing transverse momentum (or equivalently from the energy slope of the gluon multiplicity) to that of the multiplicity in e$^+$e$^-$ annihilation the colour factor ratio has been verified with small uncertainties [18]:

$$\frac{C_A}{C_F} = 2.221 \pm 0.032 \pm$$
$$0.047_{exp.sys.} \pm 0.058_{hadc.} \pm 0.075_{theo.}$$

This results is well illustrated by Fig.5 comparing the multiplicity of colour singlet gg events (extracted from three jet events) to q$\bar{\mathrm{q}}$ events. It is immediately evident that the slope for gluons is about twice as big as for quarks. The above analysis has recently been confirmed [19]. Similarly to the analysis of the multiplicity in three jet events it should be possible to connect the multiplicity in p$\bar{\mathrm{p}}$ annihilation to that in e$^+$e$^-$. However the relevant theoretical calculations are not available so far.

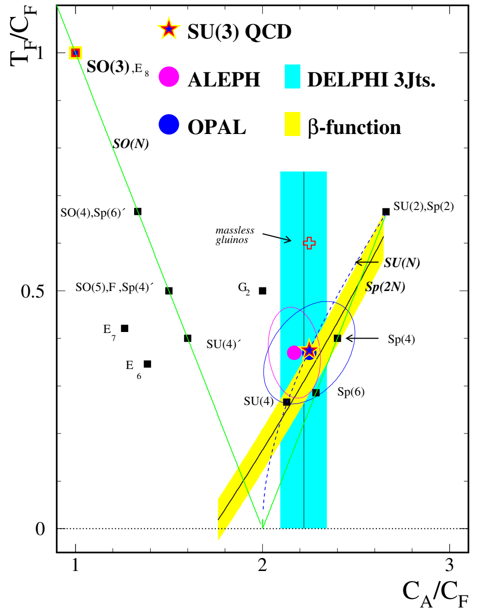

Figure 6. Constraints to the colour factors as implied by the measurements of the β–function (skewed band), the multiplicity ratio in gluon to quark jets (vertical band) and the NLO measurements from four jet events (ellipses).

The complete set of colour factors can be obtained from a measurement of events with four hard jets. There are basically three types of tree level graphs leading to four jet events: double gluon radiation ($\sigma \propto \alpha_s^2 C_F^2$) and hard gluon bremsstrahlung followed by gluon splitting into gluons ($\sigma \propto \alpha_s^2 C_F C_A$) or q$\bar{\mathrm{q}}$ ($\sigma \propto \alpha_s^2 C_F T_F$), respectively. Due to the general helicity structure of the cross–section this measurement extends also to groups other than SU(3). The initial measurements attempted to reconstruct the angular correlation between the primary quarks and the secondary partons (g or q). As the initial hard gluon is polarised (like any emitted vector particle would be) the secondary gluons (quarks) are mainly aligned along (perpendicular) to the primary quarks, respectively. A discrimination of double gluon bremsstrahlung is possible by the, in this case large angle between the gluons.

The jets are reconstructed using jet algorithms. The connection of the jets to the underlaying partons (g/q) is in general given by energy ordering. The tagging purity can be enhanced using tagging of heavy quark jets[20]. Initially the colour factor ratios C_A/C_F and T_f/C_F have been measured by the LEP experiments and SLD as the four jet cross–section was known only to leading order. Some bias is inevitable in the measurement due to the reconstruction of jets and the necessity to apply hadronisation corrections. This bias can partly be avoided by analyses using power corrections[2], however in the calculation of the power expressions connecting different observables also QCD assumptions enter.

Today the detailed structure of the cross–section is known in NLO [21]. Although the helicity arguments applied in the initial tree level analyses stay valid the recent analyses[22,23] only implicitly refer to the angular correlations. The colour factors as well as the strong coupling are inferred from a fit to the four (and three) jet cross–section as (1-dim.) function of several jet-jet angular distributions. The combined result of the measurements[22,23] yields:

$$\begin{aligned} C_A &= 2.95 \pm 0.12 \pm 0.49_{syst.} \\ C_F &= 1.34 \pm 0.06 \pm 0.49_{syst.} \end{aligned} \tag{11}$$

For this combination systematic errors have been assumed to be fully correlated. Note also that the results for C_A and C_F are strongly correlated. The results for the colour factor ratios with the 68% confidence contours are shown in Fig.6 together with the expectation of several gauge groups. These results as well as the direct determination of the colour factors are in very good agreement with QCD (SU(3)) expectation.

4. Summary

Stringent and successful precision tests of QCD have been discussed. The multiplicity ratio in gluon to quark jets and the angular distribution of four jet events confirm the relative coupling strength of the QCD vertices and thereby the gauge group underlaying strong interactions (see Fig. 6). The energy evolutions of the b quark mass and the event shape means provide detailed tests of the QCD quantum corrections. The basic measurement of the β–function excludes hypothetical light gluinos (see Fig. 6).

REFERENCES

1. Talk by D. Ward, these proceedings.
2. Talk by S. Kluth, these proceedings.
3. DELPHI Collab., R. Reinhard *et al.*, contribution to EPS HEP 2001, Budapest, DELPHI 2001-062 Conf 490.
4. A. Dhar, Phys. Lett. B **128**, 407 (1983).
5. A. Dhar and V. Gupta, Pramana **21** (1983) 207, Phys. Rev. D **29**, 2822 (1984).
6. W. Celmaster and R.J. Gonzalves, Phys. Rev. D **20**, 1420 (1979).
7. M. Beneke, Phys. Lett. B**307**,154 (1993).
8. J.M. Campbell *et al.*, Phys. Rev. Lett., **81**, 1568, (1998).
9. E. L. Berger *et al.*, Phys. Rev. Lett. **86** (2001) 4231.
10. DELPHI Collab., P. Abreu *et al.*, Phys. Lett. B **418** (1998) 430.
11. ALEPH Collab., R. Barate *et al.*, Eur. Phys. J. C **18** (2000) 1
12. OPAL Collab., G. Abbiendi *et al.*, Eur. Phys. J. C **21** (2001) 411
13. A. Brandenburg et al., Phys. Lett. B **468** (1999) 168
14. J. Fuster, talk given at QCD@work, Martina Franca, Italy, June 2001.
15. DELPHI Collab., P. Abreu *et al.*, Z. Phys. C **70** (1996) 179.
16. DELPHI Collab., P. Abreu *et al.*, Phys. Lett. B, **449** (1999) 383.
17. P. Eden, JHEP **9809** (1998) 015.
18. DELPHI Collab., K. Hamacher *et al.* , CERN-OPEN-2000-134.
19. OPAL Collab., G. Abbiendi *et al.* ,hep-ex/0111013.
20. DELPHI Collab., P. Abreu *et al.* Phys. Lett. B **414**, 401 (1997).
21. L. J. Dixon and A. Signer, Phys. Rev. D **56** (1997) 4031, Z. Nagy and Z. Trocsanyi, Phys. Rev. D **59**, 14020 and D **62**, 99902 (1999) .
22. OPAL Collab., G. Abbiendi *et al.* ,Eur. Phys. J. C **20** (2001) 601
23. ALEPH Collab., S. Bravo, *et al.* , Aleph 2001-41, contribution to EPS HEP 2001, Budapest.